Battery State-of-Charge Estimation Prototype using EMF Voltage Prediction

Christoph Unterrieder*, Michael Lunglmayr*, Stefano Marsili** and Mario Huemer†

*Institute of Networked and Embedded Systems
Klagenfurt University, 9020 Klagenfurt, Austria
Email: christoph.unterrieder@aau.at
**Infineon Technologies Austria AG
9500 Villach, Austria
†Institute of Signal Processing
Johannes Kepler University Linz, 4040 Linz, Austria

Abstract—A reliable knowledge of cell parameters like the state-of-charge (SoC) is essential for the optimization of battery-powered applications. Usually, during relaxation (the phase of no or low loads) the SoC is determined based on the measurement of the battery's electro-motive force (EMF). To obtain a reliable measurement, it is required that the battery voltage transient is in a well-relaxed state, which is rarely reached in practice (e.g. due to periodic discharge activities). In this paper, a predictive methodology is presented which is able to forecast the EMF and therewith the SoC already during a not well-relaxed state of the voltage transient. A nonlinear relaxation voltage model is reformulated such that the problem can be treated as a linear least squares estimation problem. Based on this estimation, the performance is evaluated with respect to the following aspects: prediction time, current rate influence, SoC influence, cell-to-cell deviation, or rather aging and temperature effects. Experimental results are presented for a fixed-point implementation of the estimation scheme on a CY8CKIT-050 PSOC5 programmable system on chip. For validation, measurements of $2.25\,\mathrm{A\,h}$ Sanyo UR18650A lithium cells have been used. It is shown that the presented approach offers an improved re-initialization methodology for the Coulomb counting method, and that it clearly outperforms the usual EMF-measurement based SoC determination method.

I. INTRODUCTION

In the recent years, the demand on sophisticated battery management solutions for battery-powered devices has significantly increased. In the last decade, improving the utilization of the available cell capacity and increasing the battery runtime has become an important research focus in the community. For that, a reliable knowledge of internal cell parameters like the state-of-charge (SoC) is a crucial requirement. State-of-the-art implementations of battery fuel gauge integrated circuits (FG ICs) are mainly based on two concepts [1], [2]:

Coulomb counting: The amount of charge during a charge or discharge phase is estimated by the integration of the measured current rate over time. Adversely are the errors introduced by the sampling process, the time-varying input offset of the analog-to-digital converter (ADC), as well as the uncertainty in the initial SoC and the capacity of the battery.

Open-circuit voltage (OCV) measurement: The Coulomb counting method is re-initialized based on a predefined SoC-OCV relationship. For this, the cell voltage transient is required to be in a well-relaxed state. In practice, this state is assumed to be reached when the charge or discharge current is below a specific threshold value I_{th} for a specific time period T_{relax} (typical values are: $I_{\mathrm{th}} \leq 0.1\,\mathrm{C-rate}$ and $T_{\mathrm{relax}} \geq 30\,\mathrm{min}$). Alternatively, the well-relaxed state can be supposed to be reached if the temporal change of the relaxation voltage transient drops below a pre-defined value (e.g. $\leq 3\,\mu\mathrm{V\,s}^{-1}$). For the OCV-based determination of the SoC, in practice usually a fixed, age-independent OCV-SoC relationship is assumed for the battery.

Unfortunately, the OCV does not promptly coincide with a cell's electro-motive force (EMF) when entering the relaxation phase [1]-[3]. With ongoing time, the OCV converges to the EMF. The convergence time (T_{cvg}) strongly depends on parameters like the SoC, the temperature (T) or the applied charge (I_{chg}) or discharge (I_{dchg}) current rate. Potentially, $T_{\mathrm{cvg}} \geq T_{\mathrm{relax}}$, which is not taken into account appropriately in most of today's battery fuel gauge implementations. Recently, also predictive SoC estimation methodologies have been proposed, which are capable of predicting the SoC based on a forecast of the OCV during relaxation [4]-[6]. In [7], [8], impedance-based battery descriptions are used to estimate the EMF. In the past, also model-based SoC estimation methods have been published in literature [9]-[13]. Those are used to compensate for errors which are introduced by the Coulomb counting method. Exemplary methodologies are based on the Kalman- or the H_{∞}-filter [9]-[11], the Luenberger observer or the sliding mode observer [11]-[13]. These methods require a realistic cell model, which is difficult to extract for the variety of existing use cases and operating conditions.

In this work, it is shown that a nonlinear battery relaxation voltage model can be reformulated such that the problem can be treated as a linear least squares (LS) estimation problem. The estimation performance is evaluated with respect to parameters like the prediction time, the current rate, the SoC, the temperature, cell-to-cell deviations, and the battery aging. Experimental results are presented based on the measurements

of Sanyo UR18650A lithium cells, and based on the implementation of the estimation scheme on a CY8CKIT-050 PSOC5 programmable system on chip. In Section II, the concept of the proposed methodology, and details about the used relaxation model are presented. Section III presents experimental results and validates the presented concept with respect to different influence factors. Section IV concludes the paper.

II. CONCEPT

In this section, the used relaxation voltage model and the concept of the proposed EMF prediction method are presented.

A. Modeling of the voltage relaxation process

Recently, a voltage model based ordinary LS estimation approach has been proposed to predict the prospective OCV of a battery relaxation phase. Based on the forecast of the OCV, the battery's SoC is estimated. For the estimation process, voltage samples from the early phase of the relaxation phase are used. The OCV transient is modeled by [3]

$$V_{\mathrm{b}}(t) = V_{\mathrm{o}} - \frac{\Gamma\gamma}{t^{\alpha} \log_{e}^{\delta}(t)} \cdot e^{\varepsilon_t/2}, \qquad (1)$$

where the parameters to be estimated are given by γ, α, $\delta > 0$ (rate-determining constants) and V_{o}. Γ equals to ± 1, depending on an occurring relaxation after charge or discharge. ε_{t} represents a random error term with an exponential multiplicative error structure, and t indicates the instant of time with respect to the starting point of the battery relaxation phase. The validity of (1) has been proven based on the application of a nonlinear LS estimator, where for the chemistry under test the OCV transients have been evaluated with respect to the goodness of fit for different operating conditions. In [3], V_{o} is denoted as the end value of the relaxation phase. In this work we demonstrate that V_{o} in (1) might not always be the best candidate for predicting the end value of the corresponding battery voltage relaxation process. Obviously there exist combinations of the parameters to be estimated for which the time-dependent part $V_d(t)$ in (1), given by

$$V_d(t) = \frac{\Gamma\gamma}{t^{\alpha} \log_{e}^{\delta}(t)}, \qquad (2)$$

does not converge to zero. This is equivalent to the fact that the battery's OCV does not converge to V_{o} with ongoing time. Thus, the end value of the voltage relaxation process can be written as

$$V_b(\infty) = V_{\mathrm{o}} - a, \qquad (3)$$

where V_{o} differs from $V_b(\infty)$ by a non-zero offset a. Based on (3), we propose to not use V_{o} for the prediction of the relaxation end value in (1). In the next step, we demonstrate based on Fig. 1 that the characteristic of the battery voltage relaxation process strongly depends on the temperature, the SoC, and the battery aging. In Fig. 1 (a) the battery voltage characteristic for a pulse discharge scenario is plotted, obtained by measurements at $T = 10\,°\mathrm{C}$, starting at a fully charged state to show different behaviors at different SoCs. The battery has been discharged in 5% steps of SoC (at $0.1\,\mathrm{C}$–rate), followed by a period of rest ($0\,\mathrm{A}$), respectively. The resting periods have been aborted as soon as the temporal change of the battery voltage has dropped below $3\,\mathrm{\mu V\,s^{-1}}$, respectively. From that

it can be concluded that the transients around $25 - 35\%$ SoC, as well as around $60 - 80\%$ SoC are reaching their well-relaxed state much slower compared to the transients at the remaining SoCs. This behavior has not been observed for high temperatures ($30\,°\mathrm{C}$), but it becomes more and more present for decreasing temperatures. This is mainly caused by diffusion limitations of the involved electro-chemical reactions [1]. In order to describe this behavior in terms of an electric quantity, the battery resistance $R_{\mathrm{b,relax}}$ is introduced. It describes the battery voltage gain during the relaxation phase in dependency of the current rate value of the preceding charge or discharge phase. In Fig. 1 (b), the characteristic of $R_{\mathrm{b,relax}}$ is illustrated dependent on the temperature, the SoC, the aging (cycle number N) and the cell-to-cell deviation. The data has been obtained based on characterization. As we are interested in the long term trend of V_b, the first $100\,\mathrm{s}$ of the relaxation process have been neglected for the extraction of $R_{\mathrm{b,relax}}$. It can be concluded that both a decreased temperature and an increased cycle number result in an increased value of $R_{\mathrm{b,relax}}$, as expected. Interestingly, also the peaks around $25 - 35\%$ SoC and around $60 - 80\%$ SoC are higher at low temperatures. This is directly related to the speed of the relaxation voltage transients at these SoC points. Moreover, we observed that cell-to-cell deviations play just a minor role.
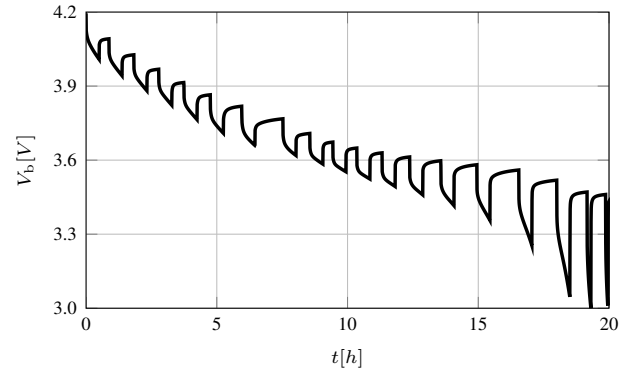
(a) Voltage characteristic, $T = 10\,°\mathrm{C}$.
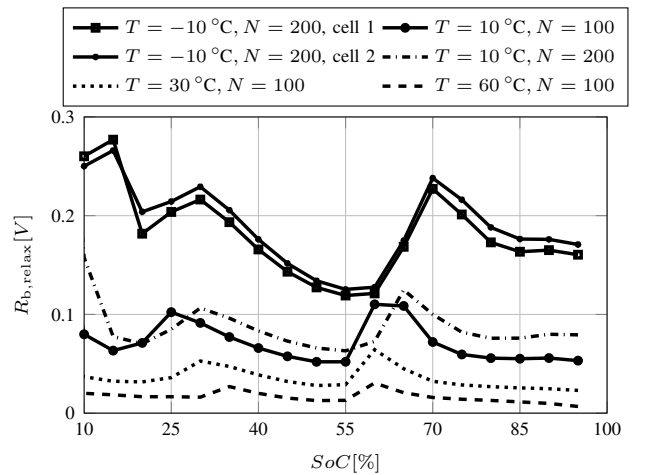
(b) Impedance characteristic.

Fig. 1: Battery characterization.

B. Estimation scheme

Although the model in (1) is non-linear in its parameters, below we show a way to formulate the estimation process via a linear LS problem. By squaring (1), and by applying the logarithm on both sides of the squared version of (1), one gets

$$\left(\frac{\Gamma\gamma}{t^\alpha \log_e^\delta(t)}\right)^2 = (V_o - V_b(t))^2 \cdot e^{-\varepsilon_t},$$

$$\log_e (V_o - V_b)^2 = C + A\log_e(t) + D\log_e(\log_e(t)) + \varepsilon_t, \tag{4}$$

with $\Gamma = +1$ (discharge scenario), and A, C and D given by

$$C = 2\log_e(\gamma), \tag{5}$$
$$A = -2\alpha, \tag{6}$$
$$D = -2\delta. \tag{7}$$

With $\boldsymbol{\theta} = (C, A, D)^T$, $t_i = t_1, ..., t_N$, $y_{t_i}(V_b(t_i), V_o) = 2\log_e(V_o - V_b(t_i))$ and $\mathbf{h}_{t_i} = [1, \log_e(t_i), \log_e(\log_e(t_i))]^T$, this can be formulated in a linear form as

$$y_{t_i}(V_b(t_i), V_o) = \mathbf{h}_{t_i}^T\boldsymbol{\theta} + \varepsilon_{t_i}. \tag{8}$$

t_i denote the points in time at which measurements of the battery voltage $V_b(t_i)$ are recorded during relaxation. For a fixed guess of V_o, $\boldsymbol{\theta}$ could in principle be estimated by a linear LS estimator. One approach is the use of the LS batch solution (e.g. via a pseudo inverse calculation), where the calculation would require that all measurements which are to be considered for the estimation process are already available. This would lead to an LS solution which minimizes the LS cost function with respect to a particular choice of V_o. Theoretically, V_o could be found by performing a grid search on V_o, which would require to solve the linear LS problem for each potential V_o on the grid. Clearly, this approach is not feasible in practical implementations. In this work, we propose the use of a modified sequential LS estimation strategy, which iteratively updates the estimate $\hat{V}_o$ of V_o by the use of $\hat{\boldsymbol{\theta}}$. Continuative, the estimation error is reduced step by step based on the adjustment of $\hat{\boldsymbol{\theta}}$ and $\hat{V}_o$. Thereby, $\hat{\boldsymbol{\theta}}$ is updated iteratively based on the sequential LS estimation procedure, given by

$$\hat{\boldsymbol{\theta}}_{t_i} = \hat{\boldsymbol{\theta}}_{t_{i-1}} + \boldsymbol{K}_{t_i} \cdot \left[y_{t_i}(V_b(t_i), \hat{V}_{o,t_{i-1}}) - \mathbf{h}_{t_i}^T\hat{\boldsymbol{\theta}}_{t_{i-1}}\right], \tag{9}$$

$$\boldsymbol{K}_{t_i} = \frac{\boldsymbol{\Sigma}_{t_{i-1}}\boldsymbol{h}_{t_i}}{1 + \boldsymbol{h}_{t_i}^T\boldsymbol{\Sigma}_{t_{i-1}}\boldsymbol{h}_{t_i}}, \tag{10}$$

$$\boldsymbol{\Sigma}_{t_i} = (\mathbf{I} - \boldsymbol{K}_{t_i}\boldsymbol{h}_{t_i}^T) \cdot \boldsymbol{\Sigma}_{t_{i-1}}. \tag{11}$$

$\boldsymbol{K}_{t_i} \in \mathbb{R}^{3\times1}$ denotes the so-called gain matrix and $\boldsymbol{\Sigma}_{t_i} \in \mathbb{R}^{3\times3}$ defines a temporary matrix which is required for updating $\boldsymbol{K}_{t_i}$. $\hat{\boldsymbol{\theta}}$ can be initialized via the zero vector. $y_{t_i}(V_b(t_i), \hat{V}_{o,t_{i-1}})$ represents the "measurement" for the estimation process, where $\hat{V}_{o,t_{i-1}}$ is the best available estimate of V_o, calculated at time instant t_{i-1}. $\hat{V}_o$ is initialized based on an initial guess. For this work we used $\hat{V}_{o,t_0} = V_{b,0} + 0.25$ V as initial value, where $V_{b,0}$ is obtained by the measurement of the cell voltage at the start of the relaxation process [3]. After every sequential LS update, an updated value for $\hat{V}_{o,t_i}$ can be iteratively found based on $\hat{y}_{t_i}$, given by

$$\hat{V}_{o,t_i} = V_b(t_i) + e^{\hat{y}_{t_i}/2}. \tag{12}$$

(12) is found based on the deformation of the term $\hat{y}_{t_i}(V_b(t_i), \hat{V}_{o,t_i}) = 2\log_e(\hat{V}_{o,t_i} - V_b(t_i))$. By iteratively solving (9)-(12), new estimates of C, A and D are available at each time instant t_i. According to (5), (6) and (7), updated values for γ, α and δ can be extracted for t_i. Based on (5), (6), (7) and (12) we can now evaluate (1) for an arbitrary point in time. As we want to estimate the battery's EMF, the evaluation point in time T_{eval} can be chosen dependent on operating conditions like the temperature or the SoC. For easy comparison, we choose $T_{eval} = 3$ h. Thereby, it is assumed that after 3 h the battery has reached its EMF (an assumption that was validated by lab measurements).

III. EXPERIMENTAL RESULTS

In this section, the experimental results of the proposed EMF prediction method are presented based on measurements of 2.25 Ah Sanyo UR18650A lithium cells. Similar results have been obtained for the application of the proposed methodology to batteries with other cell chemistries. The estimation scheme has been implemented on a CY8CKIT-050 PSOC5 programmable system on chip in 16 bit fixed-point arithmetic. In Fig. 2 (a), the prediction result for a single OCV relaxation curve at 25% SoC is plotted. Prior to the no-load relaxation phase, a 30 min lasting discharge period has been applied ($I_{dchg} = 0.1$ C–rate). The black dashed line represents the measured OCV relaxation curve, denoted by $V_b(t)$. The black and the gray solid lines show the end value of the relaxation process $V_b(\tau = 3$ h), plus some pre-defined threshold values ($i.e. \pm 2$ mV). These chemistry-dependent threshold values are defined by the requested SoC estimation accuracy and are extracted based on the SoC-OCV relationship of the battery under test. The black dash-dotted line represents the predicted EMF value, obtained by the application of the proposed estimation scheme. Thereby, (1) has been evaluated for $T_{eval} = 3$ h, yielding $\hat{V}_b(T_{eval})$. t_i has been set to $t_i = [120 + k \cdot 100]$ s, with $k \in \mathbb{N} \cup \{0\}$. From Fig. 2 (a) it can be concluded that by applying the proposed prediction scheme, a reliable estimate of the relaxation end value is available much earlier as this is the case by relying on the OCV measurement. For the considered case, the predicted EMF curve is within the specified accuracy of ± 2 mV after $T_{pred} = 8$ min. Contrary the measured OCV curve lies within the specified threshold region after around $T_{meas} = 80$ min. Resting periods of 80 min occur rarely in today's applications. In contrast, 8 min lasting relaxation periods may appear regularly in practice. The proposed prediction scheme allows reducing the time intervals between re-initializing the Coulomb counting method and thus increasing its accuracy. Capacity tracking algorithms often rely on the availability of successional relaxation phases. Thus, the proposed methodology also increases the frequency with which the capacity of the battery can be estimated.

In Fig. 2 (b), T_{meas} and T_{pred} are compared over the entire range of the SoC, gathered for $I_{dchg} = 0.1$ C–rate, $T = 30$ °C and $N = 100$ or rather $N = 200$ (to show effects of battery aging). The gray ($N = 100$) and the black ($N = 200$) circle-marked data points represent the needed time until the OCV measurement reaches a specified accuracy of 1% (1% in terms of SoC). The squared-marked data points are showing the equivalents for using the proposed EMF prediction procedure. It can be concluded that the EMF prediction method

outperforms the OVC measurement based methodology in all SoC points, or at least yields the same performance as e.g. for $SoC = 80\%$. As expected, T_{pred} is raising for increased values of T_{meas}. This means that if the speed with that the transient of the relaxation phase reaches its well-relaxed state is getting slower, then the time needed for the prediction process is increasing (the time to reach a reliable estimate at the specified accuracy increases). By comparing Fig. 1 (b) and Fig. 2 (b), we conclude that increased values of T_{meas} especially occur for SoC regions in which $R_{\mathrm{b,relax}}$ has high values. In general, aging causes the battery impedance to get increased, which on the other hand implicates a slowdown of the speed with which the transients get relaxed. Interestingly, for $SoC = 60\%$ and $SoC = 30\%$, the relaxation transients accelerate with aging.
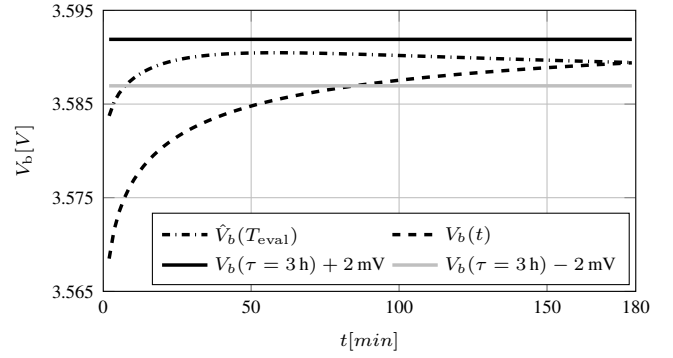
In Fig. 2 (c), T_{meas} and T_{pred} are compared for $T = 10\,°\mathrm{C}$. In general, a decrease of the operating temperature implicates a slowdown of the speed with that the transients get relaxed. This is confirmed by the fact that for $T = 10\,°\mathrm{C}$, the values of T_{meas} are in general much higher compared to the case of $T = 30\,°\mathrm{C}$ in Fig. 2 (b). On the other hand, at low temperatures the proposed EMF prediction methodology offers an increased gain with respect to the achievable SoC estimation accuracy compared to the state-of-the-art method. Aging causes the battery impedance to be increased, which on the other hand implicates a slowdown of the speed with that the transients get relaxed. At $SoC = 25\%$ and $SoC = 60\%$, again the opposite behavior has been observed. For higher current rates, it was observed that in general T_{pred} increases.
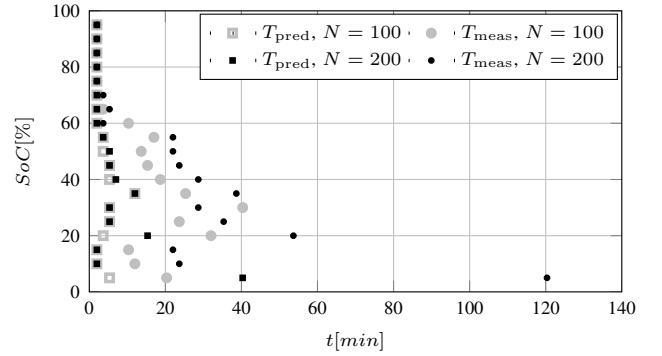
IV. CONCLUSION

A methodology has been presented that is able to predict a battery's EMF already in a not well-relaxed state of the OCV transient. This may be utilized to re-initialize the Coulomb counting method and to update the battery's capacity information more frequently and accurately as this can be done by state-of-the-art methods. Re-initializing the Coulomb counting method is important in the presence of initial SoC or battery capacity uncertainties, or measurement errors. The proposed approach is based on an extended sequential linear least squares estimation scheme applied to a nonlinear relaxation voltage model. The proposed estimation scheme has been implemented on a CY8CKIT-050 PSOC5 programmable system on chip to demonstrate its capabilites in real world scenarios. The evaluation is done with respect to influence factors like the SoC, the temperature and the battery aging. Experimental results are presented for measurements of Sanyo UR18650A lithium cells. It is shown that the proposed methodology clearly outperforms the typically used OCV-measurement method.

(a) EMF prediction, $T = 10\,°\mathrm{C}$, 25% SoC, $I_{\mathrm{dchg}} = 0.1\,\mathrm{C}$.

(b) T_{pred} vs. T_{meas}, $T = 30\,°\mathrm{C}$, $N = 100/200$ and $I_{\mathrm{dchg}} = 0.1\,\mathrm{C}$.

(c) T_{pred} vs. T_{meas}, $T = 10\,°\mathrm{C}$, $N = 100/200$.

Fig. 2: EMF prediction: Results.

REFERENCES
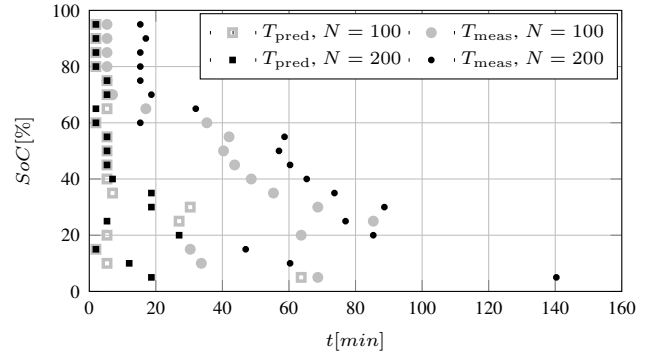
[1] V. Pop, HJ. Bergveld, PHL. Notten and PPL. Regtien, 'State-of-the-art of battery state-of-charge determination', *Measurement Science and Technology*, Vol. 16, No. 12, pp. R93-R110, 2005.

[2] S. Piller, M. Perrin, and A. Jossen, 'Methods for state-of-charge determination and their applications', *Journal of Power Sources*, Vol. 96, No. 1, pp. 113-120, 2001.

[3] V. Pop et al., *Battery management systems: Accurate state-of-charge indication for battery-powered applications*, Springer Verlag, Philips Research Book Series, Volume 9, Eindhoven 2008.

[4] C. Unterrieder, M. Lunglmayr, S. Marsili and M. Huemer, 'Battery state-of-charge estimation using polynomial enhanced prediction', *IET Electr. Letters*, Vol. 48, No. 21, pp. 1363-1365, 2012.

[5] C. Unterrieder, R. Priewasser, S. Marsili and M. Huemer, 'Comparative study and improvement of battery open-circuit voltage estimation methods', *Proc. IEEE Mid. Symp. on Circuits and Systems (MWSCAS)*, pp. 1076-1079, Boise, USA, 2012.

[6] C. Unterrieder, M. Lunglmayr, S. Marsili and M. Huemer, 'Computer-aided Optimization for Predictive Battery State-of-charge Determination', *Lecture Notes in Computer Science (LNCS): Computer Aided Systems Theory - EUROCAST 2013*, Vol. 8111, pp. 476-482, 2013.

[7] W. Waag, D.U. Sauer, 'Adaptive estimation of the electromotive force of the lithium-ion battery after current interruption for an accurate state-of-charge and capacity determination', *Applied Energy*, Vol. 111, pp. 416-427, 2013.

[8] M. Coleman et al., 'State-of-Charge Determination From EMF Voltage Estimation: Using Impedance, Terminal Voltage, and Current for Lead-Acid and Lithium-Ion Batteries', *IEEE Transactions on Industrial Electronics*, Vol. 54, No. 5, pp. 2550-2557, 2007.

[9] G.L. Plett, 'Extended Kalman filtering for battery management systems

of LiPB-based HEV battery packs', *Journal of Power Sources*, Vol. 134, pp. 252-292, 2004.

[10] C.P. Bhuvana, C. Unterrieder and M. Huemer, 'Battery Internal State Estimation: A Comparative Study of Non-Linear State Estimation Algorithms', *Proc. IEEE Vehicular Power and Propulsion Conference (VPPC)*, Beijing, China, pp. 65-70, Oct. 2013.

[11] C. Unterrieder, R. Priewasser, S. Marsili and M. Huemer, 'Battery state estimation using mixed Kalman/H_∞, adaptive Luenberger and sliding mode observer', *Proc. IEEE Vehicular Power and Propulsion Conference (VPPC)*, Beijing, China, pp. 71-76, Oct. 2013.

[12] X. Hu, F. Sun and Y. Zou, 'Estimation of State of Charge of a Lithium-Ion Battery Pack for Electric Vehicles Using an Adaptive Luenberger Observer', *Energies*, Vol. 3, No. 9, pp. 1586-1603, 2010.

[13] IS. Kim, 'The novel state of charge estimation method for lithium battery using sliding mode observer', *Journal of Power Sources*, Vol. 163, No. 1, pp. 584-590, 2006.